

On the Evaluation of Critical Lateral-Torsional Buckling Loads of Monosymmetric Beam-Columns

T. Yilmaz, N. Kirac

Abstract—Beam-column elements are defined as structural members subjected to a combination of axial and bending forces. Lateral torsional buckling is one of the major failure modes in which beam-columns that are bent about its strong axis may buckle out of the plane by deflecting laterally and twisting. This study presents a compact closed-form equation that it can be used for calculating critical lateral torsional-buckling load of beam-columns with monosymmetric sections in the presence of a known axial load. Lateral-torsional buckling behavior of beam-columns subjected to constant axial force and various transverse load cases are investigated by using Ritz method in order to establish proposed equation. Lateral-torsional buckling loads calculated by presented formula are compared to finite element model results. ABAQUS software is utilized to generate finite element models of beam-columns. It is found out that lateral-torsional buckling load of beam-columns with monosymmetric sections can be determined by proposed equation and can be safely used in design.

Keywords—Lateral-torsional buckling, stability, beam-column, monosymmetric section.

I. INTRODUCTION

BEAM-COLUMNS are members with compressive axial forces and transverse loads or moments. Beam-columns are mostly loaded in the plane of the weak axis so that bending occurs about their strong axis [1]. Primary bending moments and in-plane deformations are produced by the end moments and transverse loadings of the beam-column, while axial force will produce secondary moments and additional in-plane deformations [1]. When the values of the loads on the beam-column reach a limiting state, the member will experience out of plane bending and twisting [1]. At this critical state, the compression flange of the member becomes unstable and bends laterally while the remainder of the cross section, which is stable, tends to restrain the lateral flexure of the compression flange. The net effect is that the whole section rotates and moves laterally [2]. LTB failure occurs suddenly in slender beam-columns with a much greater in-plane bending stiffness than their lateral bending or torsional stiffnesses [1]. LTB is often the main failure mode for thin-walled structures and should be considered in design of slender beam-columns with insufficient lateral bracing due to it may occur long before the bending stress at the extreme fiber of the section reaches to yield point. Fig. 1 illustrates LTB of beam-column with I-section.

T. Yilmaz and N. Kirac are with the Department of Civil Engineering, Eskisehir Osmangazi University, Eskisehir, Turkey (e-mail: tyilmaz@ogu.edu.tr, kiracn@ogu.edu.tr).



Fig. 1 LTB of beam-column with I-section

The limit state of the applied loads on the beam-column members is called as the critical elastic LTB load. The cross section of the member, the unbraced length of the member, the support conditions, the type of loads acting on the member, the vertical positions of the applied loads with respect to shear center are effective on LTB behavior of monosymmetric beam-columns. The general concept of flexural buckling and LTB of structural members has been well presented in many textbooks [3]-[9].

There are three main methods to calculate the critical elastic LTB load. The first one is the solution of the differential equilibrium equations. The differential equilibrium equations obtained for critical LTB load of an axially loaded beam subjected to end moment about its major axis can be solved and presented in closed form by considering the boundary conditions [9]-[11]. However, the analytical solutions are either too complex or involve infinite series for load types where moment gradient is not constant. In a situation like this, the solution of differential equilibrium equations mostly requires use of numerical approaches such as finite difference [2], [12]-[15], finite integral [16]-[19], finite element [20]-[29] or finite strip [30]-[33] methods. The second one is finite element analysis (FEA). In FEA, thin walled structural member, restraint conditions and loading cases should be modeled properly and solved using a relevant FEA software [34]. The last one is energy method. Energy method is based on the equality between the additional strain energy stored during LTB and the additional work done by the applied forces. In this method, the LTB load is calculated by substituting an approximate buckled shape which satisfies the kinematic boundary conditions and corresponds to real mode

shape into the energy equation. Kinematic boundary conditions are related to geometrical constraints preventing one or more deflections or rotations at the support of the structural members [9].

A considerable number of studies dealing with the energy methods exist in the literature. Wang and Kitipornchai studied LTB of monosymmetric cantilevers using both the Ritz method and the finite integral method [35]. They proposed the approximate equation to calculate LTB of cantilevers subjected to the end moment, the end point load and uniformly distributed load. Aydin et al. investigated the LTB loads of both mono-symmetric and doubly-symmetric prismatic beams for various load cases and positions of applied loads [36]. In this work, the obtained results by the energy method were validated with ABAQUS FEA and compared with Eurocode 3 [37] and AISC Specifications [38]. Mohri et al. recomputed 3-factor formula, which is commonly used for calculation of elastic LTB loads of beams, and proposed some improvements [39]. Kirac and Yilmaz introduced a simplified parametric equation to determine LTB load of European I-section beams [40]. The LTB loads of singly and doubly symmetric I-section cantilevers were investigated by Andrade et al [41]. Ozbasaran et al. developed an alternative design procedure for cantilever I-section and also the study included a parametric formula based on energy method to calculate LTB load. The proposed design procedure was compared with code specifications and FEA [42]. Yuan et al. improved an analytical model to determine LTB behavior of steel web tapered tee-section cantilevers [43]. Kim et al. studied LTB of castellated beams [44]. LTB of simply supported channel and Z section purlins with top flange horizontally restrained are investigated by Zhang and Tong [45]. LTB of tapered thin-walled beams with arbitrary cross section are presented by Mohri et al [46].

Related to LTB of beam-columns, Wang and Kitipornchai proposed a set of buckling parameters to describe LTB behavior of monosymmetric beam-columns under uniform moment or eccentric axial loads [47]. Torkomani and Roberts derived the energy equations for doubly symmetric beam-column members by expressing in dimensional and non-dimensional forms [1]. Magnucka-Blandzi investigated beam-columns with I-section subjected to a uniformly distributed transverse load, small axial force and two different moments located at its both ends [48]. Cheng et al. studied flexural buckling and LTB of cold-formed channel section beams under combined compression and biaxial bending. They also concluded the effect of non-symmetric pre-buckling stress due to bending about the minor axis distribution on LTB of channel beams [49]. Kucukler et al. introduced a stiffness reduction method for the flexural-torsional buckling assessment of steel beam-columns subjected to major axis bending and axial compression [50].

In this study, LTB behavior of beam-columns with monosymmetric section subjected to constant axial force and various transverse load cases were investigated by using energy method in order to establish a convenient closed-form equation. The coefficients of the closed-form equation are calculated for six transverse load types. The presented

equation takes into account the position of loads acting transversely on the beam-column member respect to shear center and monosymmetry property of the section, but disregards pre-buckling deflections. Numerical examples are presented for both mono-symmetric and doubly-symmetric sections by considering axial load level, loading positions and slenderness of beam-column. FEA is performed to validate numerical examples by using ABAQUS software [51]. It is seen that the results obtained by presented formula are accordant with ABAQUS solutions. It is concluded that elastic critical LTB load of beam-columns under small axial forces can be calculated by using presented equation.

II. ANALYTICAL WORK

The LTB of monosymmetric beam-columns consists of two stages. First, combined transversely and compressive axially loaded beam-column bends about its major axis, and then it buckles by bending laterally and twisting as the magnitude of the loads acting on the beam-column reaches to a critical level. Fig. 1 shows the LTB of beam-column with monosymmetric I-section subjected to axial force that acts through the centroid of the cross section and concentrated force that acts transversely at midspan.

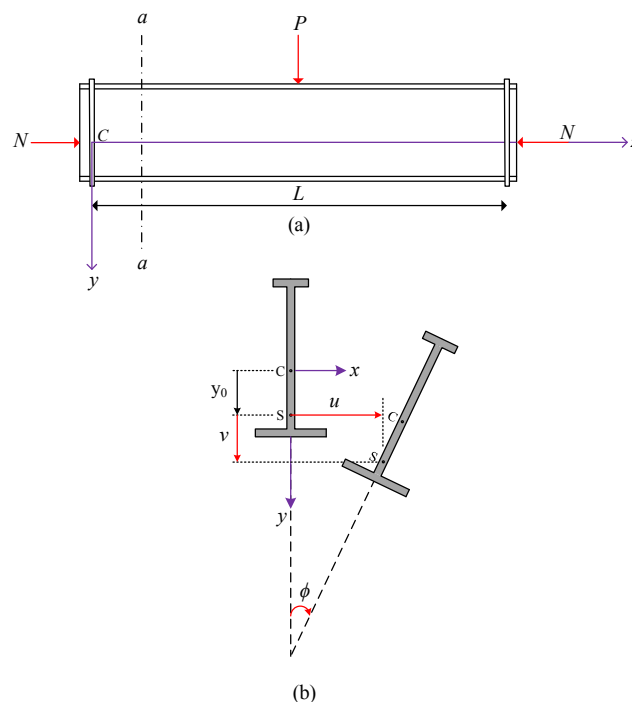


Fig. 2 LTB of mono-symmetric beam-column (a) side view, (b) a-a section

In Fig. 2 (a), L is beam-column length. $a-a$ section of beam-column is drawn in Fig. 2 (b). S and C show the shear center and the center of gravity of the section, respectively. u is the lateral displacement of the shear center, v is vertical displacement of the shear center and ϕ is torsional rotation. y_0 is the distance measured from the center of gravity to the shear center. By utilizing Vlassov's model, which assumes that the

cross section is rigid in its plane, hence there is no distortion deformation of the section and the shear deformation in the mean surface of the section are negligible [39]. The total potential energy of the beam-column given in Fig 1, at a slightly buckled configuration can be written as follows by disregarding pre-buckling deflections [9].

$$\begin{aligned} \Pi = & \frac{1}{2} \int_0^L EI_y \left(\frac{d^2 u}{dz^2} \right)^2 dz + \frac{1}{2} \int_0^L EC_w \left(\frac{d^2 \phi}{dz^2} \right)^2 dz + \frac{1}{2} \int_0^L GJ \left(\frac{d\phi}{dz} \right)^2 dz \\ & - \frac{1}{2} \int_0^L N \left[\left(\frac{du}{dz} \right)^2 + \left(\frac{I_x + I_y}{A} + y_0^2 \right) \left(\frac{d\phi}{dz} \right)^2 + 2y_0 \left(\frac{du}{dz} \right) \left(\frac{d\phi}{dz} \right) \right] dz \quad (1) \\ & + \frac{1}{2} \int_0^L M_x \left[2\phi \left(\frac{d^2 u}{dz^2} \right) + \beta_x \left(\frac{d\phi}{dz} \right)^2 \right] dz + W_h \end{aligned}$$

where E is young modulus, G is shear modulus, A is area of cross section, I_x is moment of inertia about strong axis, I_y is moment of inertia about weak axis, C_w is warping constant, J is torsional constant and M_x is the bending moment about strong axis and N is constant compressive axial load. Wanger's coefficient β_x associated with a monosymmetry property of the cross section is defined by (2) [9].

$$\beta_x = \frac{1}{I_x} \int_A y(x^2 + y^2) dA - 2y_0 \quad (2)$$

where, x and y are Cartesian coordinates of the infinitesimal area (dA). y_0 is positive when the shear center below the center of gravity. W_h is work done by loads which are acting outside of the shear center. This work results from changing of the distance between the application points of the loads and the shear center as cross section rotates. W_h can be calculated by (3) as:

$$W_h = \frac{1}{2} \sum PH_p \phi_p^2 + \frac{1}{2} \int_0^L qH_q \phi^2 dz \quad (3)$$

where H_p and H_q are the vertical distance of the acting point of the concentrated (P) and uniformly distributed loads (q) measured from the shear center, respectively. ϕ_p is torsional rotation at a point in which the concentrated load is applied. In (3), H_p and H_q are positive for loads that act in below the shear center.

With the assumption that torsional rotation is small, the second order derivative of the lateral displacement u , with respect to z can be calculated as [3]:

$$\frac{d^2 u}{dz^2} = -\frac{M_x \phi}{EI_y} \quad (4)$$

Thus, the strain energy stored in the member due to lateral bending, warping and torsion can be written as:

$$U = \frac{1}{2} \int_0^L \left(\frac{M_x \phi}{EI_y} \right)^2 dz + \frac{1}{2} \int_0^L EC_w \left(\frac{d^2 \phi}{dz^2} \right)^2 dz + \frac{1}{2} \int_0^L GJ \left(\frac{d\phi}{dz} \right)^2 dz \quad (5)$$

The work done by external transverse forces is as:

$$V_1 = \frac{1}{2} \int_0^L \frac{2(M_x \phi)^2}{EI_y} dz - \frac{1}{2} \int_0^L M_x \beta_x \left(\frac{d\phi}{dz} \right)^2 dz - W_h \quad (6)$$

The work done by constant compressive axial forces is as:

$$V_2 = \frac{1}{2} \int_0^L N \left[\left(\int_0^L \frac{M_x \phi}{EI_y} dz \right)^2 + \left(\frac{I_x + I_y}{A} + y_0^2 \right) \left(\frac{d\phi}{dz} \right)^2 - 2y_0 \left(\int_0^L \frac{M_x \phi}{EI_y} dz \right) \left(\frac{d\phi}{dz} \right) \right] dz \quad (7)$$

Finally, the critical lateral torsional buckling load is obtained from the following condition:

$$U = V_1 + V_2 \quad (8)$$

Finally, the energy equation can be written as:

$$\begin{aligned} U - V_1 - V_2 = & \frac{1}{2} \int_0^L EC_w \left(\frac{d^2 \phi}{dz^2} \right)^2 dz + \frac{1}{2} \int_0^L (GJ + M_x G_x) \left(\frac{d\phi}{dz} \right)^2 dz - \frac{1}{2} \int_0^L \frac{(M_x \phi)^2}{EI_y} dz \\ & - \frac{1}{2} \int_0^L N \left[\left(\int_0^L \frac{M_x \phi}{EI_y} dz \right)^2 + \left(\frac{I_x + I_y}{A} + y_0^2 \right) \left(\frac{d\phi}{dz} \right)^2 - 2y_0 \left(\int_0^L \frac{M_x \phi}{EI_y} dz \right) \left(\frac{d\phi}{dz} \right) \right] dz \\ & + W_h = 0 \quad (9) \end{aligned}$$

To calculate the elastic critical lateral torsional buckling load by (9), a function which satisfies the end conditions of the beam-column should be selected. This function also should be consistent with the shape of the torsional rotation for the critical lateral torsional buckling mode. Assuming that the ends of the beam-column cannot rotate about the z -axis but are free to warp, the end conditions of beam-column can be considered as [3]:

$$\phi = 0 \text{ and } \frac{d^2 \phi}{dz^2} = 0 \text{ at } z = 0 \text{ and } z = L \quad (10)$$

In this study, the function of twist angle is chosen as given in (11) due to it satisfies boundary conditions stated in (10). The energy equations were solved using this function to establish closed-form equation.

$$\phi = A \sin \frac{\pi z}{L} \quad (11)$$

Substituting the chosen twist angle function in to (9) and assuming that the vertical position of all transverse loads on the beam-column are same ($H_p = H_q = H$), the energy equation can be written in the following form:

$$\begin{aligned} D_1 \frac{R_{cr}^2 L}{N_y} + D_2 \beta_x R_{cr} + D_3 \frac{N R_{cr}^2 L}{N_y^2} + D_4 R_{cr} H \\ - \frac{\pi^2 N (I_x + I_y + A y_0^2)}{4LS} + \frac{\pi^4 EC_w}{4L^2} + \frac{\pi^2 GJ}{4L} = 0 \quad (12) \end{aligned}$$

where,

$$N_y = \frac{\pi^2 EI_y}{L^2} \quad (13)$$

In (12), R_{cr} is the critical load which can be expressed by (14) depending on the load type acting on the beam.

$$R_{cr} = P_{cr} = q_{cr}L = \frac{M_{cr}}{L} \quad (14)$$

D_1, D_2, D_3 and D_4 parameters can be calculated by integrating the chosen function for critical lateral torsional buckling mode over the beam length. Finally, buckling load can be obtained by (15) as:

$$P_{cr} = q_{cr}L = \frac{M_{cr}}{L} = \frac{N_y}{2LK_2} \left[-K_1 - \sqrt{K_1^2 - K_2\pi^2 \left[\frac{C_w}{I_y} + \frac{GJL^2}{\pi^2 EI_y} - \frac{N}{N_y} \left(\frac{I_x + I_y}{A} + y_0^2 \right) \right]} \right] \quad (15)$$

K_1 and K_2 parameters in (15) can be expressed as:

$$K_1 = \beta_2 D_2 + HD_4 \quad (16)$$

and,

$$K_2 = \frac{N}{N_y} D_3 + D_1 \quad (17)$$

In (15), P_{cr} , q_{cr} and M_{cr} are critical concentrated load, uniformly distributed load and moment, respectively. In this study, D_1, D_2, D_3 and D_4 integral parameters were calculated for six load types shown in Fig. 3 and presented in Table I.

It is clearly seen from left-hand side of (15) that the critical buckling load type varies according to considered loading case. For load case 3 in Fig. 3, the critical lateral torsional buckling load obtained from (15) is in terms of q_{cr} which implies that the critical values of uniformly distributed load and concentrated load are q_{cr} and $0.5q_{cr}L$, respectively.

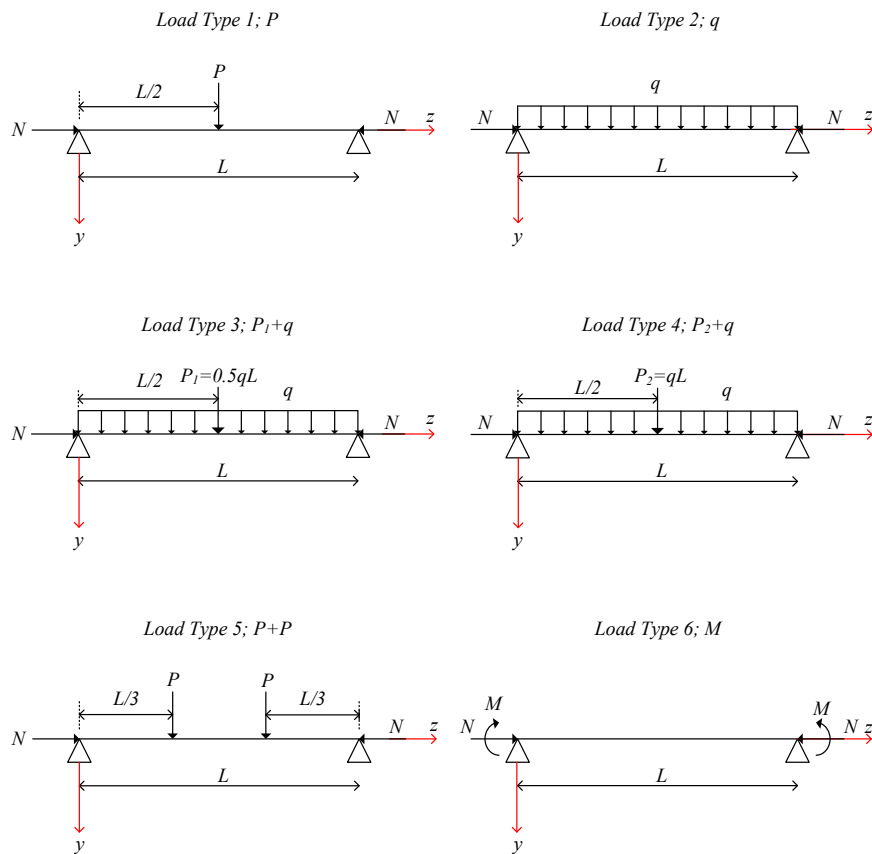


Fig. 3 Load types

TABLE I
 INTEGRAL PARAMETERS FOR LOAD CASES

Load Case	D_1	D_2	D_3	D_4
P	-0.0826542	0.183425	-0.125	0.5
q	-0.0300605	0.143117	-0.0506606	0.25
$q+0.5qL$	-0.100163	0.234829	-0.161488	0.5
$q+qL$	-0.211593	0.326542	-0.334816	0.75
$P+P$	-0.228433	0.591639	-0.221856	0.75
M	-2.4674	2.4674	-4.9348	-

At the end of the analytical work, calculating critical LTB of the beam-columns with mono-symmetric section in presence of a known axial load can be summarized in three steps. First, N_y should be calculated using (13). Then, D_1 - D_4 integral parameters can be found for considered load case in Table I. K_1 and K_2 can be calculated by using (16) and (17). Finally, critical LTB load can be found by substituting calculated parameters in closed-form (15).

III. NUMERICAL ANALYSIS

In numerical analysis, effect of axial loads, slenderness and the loading positions on the LTB loads of doubly-symmetric and mono-symmetric beam-columns are investigated. For this purpose, the analytical LTB loads are calculated for different values of the axial load by using the presented formula. The analytical solutions are compared to numerical simulations. ABAQUS finite element software was utilized to validate LTB solutions obtained by presented equation. Beam-columns were modeled with S8R5 shell elements. S8R5 element has eight-nodes and five degrees of freedom at a node [51]. Mesh studies have indicated that it would be adequate to use sixty elements along the longitudinal direction, eight elements through the depth of the web and four elements across the width of the flange [40]. Shell finite element model and buckled shapes are given in Fig. 4.

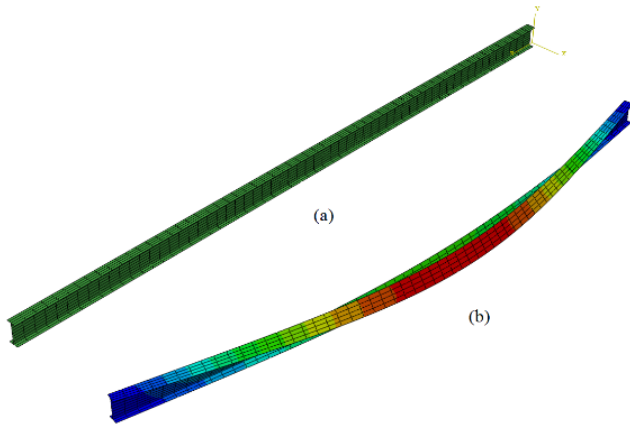


Fig. 4 (a) Shell finite element model, (b) buckled shape

Fig. 5 illustrates the sections which are used for numerical examples. Section A is a doubly-symmetric I-shape. Dimensions of Section B is similar to Section A, except width of bottom flange. The bottom flange width of Section B is reduced to half of its top flange width in order to design mono-symmetric beam-column for numerical examples. Section properties are shown in Table II.

In this numerical study, LTB loads of beam-columns were determined for three loading positions, which are top flange shear center and bottom flange in order to examine effect of load height level on LTB behavior of beam-columns. LTB loads of beam-column with section A and slenderness $L=6000$ mm are calculated for load type 1 as P and load type 4 as qL in presence of different axial load varied from $N/N_y=0$ to $N/N_y=1$. The analytical and numerical solutions are comparatively depicted for load type 1 and load type 4 in Tables III and IV, respectively.

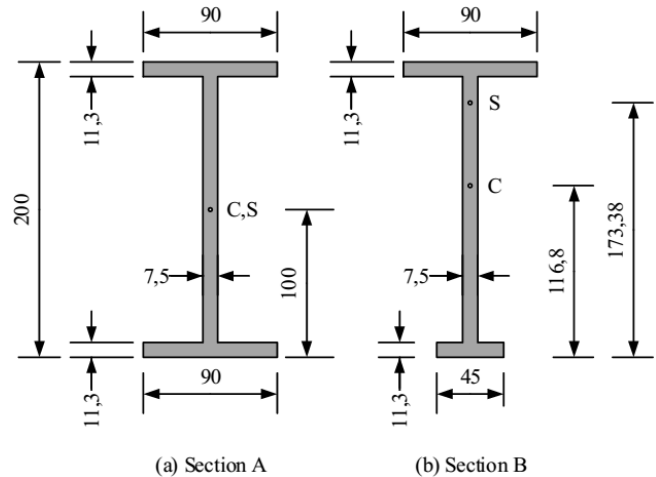


Fig. 5 (a) Section A, (b) Section B

TABLE II
SECTION PROPERTIES

Properties	Section A	Section B
t_f	11.3 mm	11.3 mm
t_w	7.5 mm	7.5 mm
b_{tf}	90 mm	90 mm
b_{bf}	90 mm	45 mm
h	200 mm	200 mm
E	200000 N/mm ²	200000 N/mm ²
G	76923 N/mm ²	76923 N/mm ²
J	113110 mm ⁴	91466.3 mm ⁴
C_w	12.222*10 ⁹ mm ⁶	2.716*10 ⁹ mm ⁶
I_x	21.618*10 ⁶ mm ⁴	16.280*10 ⁶ mm ⁴
I_y	1.379*10 ⁶ mm ⁴	0.779*10 ⁶ mm ⁴
A	3364.5 mm ²	2856 mm ²
β_x	0	131.4 mm
$^a y_0$	0	-56.6 mm

t_f = flange thickness, t_w = web thickness, b_{tf} = top flange width, b_{bf} = bottom flange width, h = section height, mm=millimeter, N=Newton. $^a y_0$ is negative when the shear center is above the center of gravity.

TABLE III
SECTION A UNDER LOAD CASE 1

Axial Load	Loading Position	PE	AB	PE/AB
$N/N_y=0$	TF	20,7	20,1	1,03
	SC	24,2	23,7	1,02
	BF	28,4	28,0	1,01
$N/N_y=0.25$	TF	17,9	17,7	1,01
	SC	20,5	20,5	1,00
	BF	23,5	23,7	0,99
$N/N_y=0.5$	TF	16,0	15,1	1,06
	SC	18,0	17,1	1,06
	BF	20,3	19,3	1,05
$N/N_y=0.75$	TF	14,6	12,5	1,17
	SC	16,2	13,9	1,17
	BF	18,1	15,5	1,17
$N/N_y=1$	TF	13,4	10,2	1,32
	SC	14,9	11,2	1,33
	BF	16,5	12,4	1,33

LTB loads are calculated for P and all units are the same as kilonewton. PE=Presented equation, AB= Abaqus, TF=Top flange, SC=Shear center, BF=Bottom flange.

TABLE IV
SECTION A UNDER LOAD CASE 4

Axial Load	Loading Position	PE	AB	PE/AB
$N/N_y=0$	TF	13,1	12,9	1,02
	SC	15,2	15,0	1,01
	BF	17,5	17,4	1,01
$N/N_y=0.25$	TF	11,2	11,1	1,01
	SC	12,7	12,9	0,99
	BF	14,4	14,7	0,98
$N/N_y=0.5$	TF	10,0	9,4	1,07
	SC	11,2	10,7	1,05
	BF	12,5	11,9	1,05
$N/N_y=0.75$	TF	9,1	7,9	1,15
	SC	10,0	8,6	1,16
	BF	11,1	9,5	1,17
$N/N_y=1$	TF	8,3	6,7	1,24
	SC	9,2	6,9	1,32
	BF	10,1	7,6	1,33

LTB loads are calculated for qL and all units are the same as kilonewton. PE=Presented equation, AB= Abaqus, TF=Top flange, SC=Shear center, BF=Bottom flange.

TABLE V
SECTION B UNDER LOAD CASE 1

Axial Load	Loading Position	PE	AB	PE/AB
$N/N_y=0$	TF	16,4	16,2	1,01
	SC	17,0	16,8	1,01
	BF	21,4	21,3	1,01
$N/N_y=0.25$	TF	13,8	14,6	0,95
	SC	14,3	15,1	0,94
	BF	17,4	18,5	0,94
$N/N_y=0.5$	TF	12,1	12,7	0,96
	SC	12,5	13,0	0,96
	BF	14,9	15,5	0,96
$N/N_y=0.75$	TF	10,9	10,6	1,03
	SC	11,2	10,8	1,03
	BF	13,2	12,5	1,05
$N/N_y=1$	TF	10,0	8,6	1,16
	SC	10,2	8,8	1,16
	BF	11,9	10,0	1,18

LTB loads are calculated for P and all units are the same as kilonewton. PE=Presented equation, AB= Abaqus, TF=Top flange, SC=Shear center, BF=Bottom flange.

TABLE VI
SECTION B UNDER LOAD CASE 4

Axial Load	Loading Position	PE	AB	PE/AB
$N/N_y=0$	TF	10,4	10,3	1,01
	SC	10,7	10,7	1,00
	BF	13,3	13,3	1,00
$N/N_y=0.25$	TF	8,7	9,3	0,94
	SC	8,9	9,5	0,93
	BF	10,7	11,5	0,93
$N/N_y=0.5$	TF	7,6	8,0	0,95
	SC	7,8	8,2	0,95
	BF	9,1	9,6	0,95
$N/N_y=0.75$	TF	6,8	6,6	1,02
	SC	6,9	6,8	1,03
	BF	8,1	7,7	1,04
$N/N_y=1$	TF	6,2	5,4	1,15
	SC	6,3	5,5	1,16
	BF	7,3	6,2	1,18

LTB loads are calculated for qL and all units are the same as kilonewton. PE=Presented equation, AB= Abaqus, TF=Top flange, SC=Shear center, BF=Bottom flange.

Tables III and IV have shown that the greatest differences between analytical results obtained by presented equation and ABAQUS solutions for Section A subjected to low axial load level ($N/N_y=0-N/N_y=0.5$) are 6% and 7% for load case 1 and load case 4, respectively. This difference becomes 33% for both load cases with high axial load level ($N/N_y=1$).

LTB loads of beam-column with section B and slenderness $L=6000$ mm are calculated for load type 1 as P and load type 4 as qL in presence of different axial load varied from $N/N_y=0$ to $N/N_y=1$. The analytical and numerical results are summarized for load type 1 and load type 4 in Table V and Table VI, respectively.

Results in Tables V and VI have shown that the greatest differences between analytical results obtained by presented equation and ABAQUS solutions for Section B subjected to low axial load level ($N/N_y=0-N/N_y=0.5$) are 6% and 7% for load case 1 and load case 4, respectively. This difference becomes 18% for both load cases with high axial load level ($N/N_y=1$). It should be noted that the ratio of analytical results obtained by presented equation to abaqus solutions have increased as 33% for section A and 18% for section B due to the fact that the increment of the axial load level after the value of $N/N_y=0.5$ invalidates the assumption for minor axis bending, which are expressed in (4).

Numerical study also includes the investigation of the effect of the slenderness on LTB behavior of beam-columns. LTB loads of section A and section B subjected to uniformly distributed load are obtained as qL by presented formula for different slendernesses varied from $L=4000$ mm to $L=10000$ mm, in presence of constant axial load of $N/N_y=0.25$ and $N/N_y=0.5$. Analytical results and ABAQUS solutions are summarized in Tables VII, VIII for section A and Tables IX and X for section B.

TABLE VII
SECTION A UNDER LOAD CASE 2 FOR $N/N_y=0.25$

L	Loading Position	PE	AB	PE/AB
4000	TF	66,6	67,7	0,98
	SC	78,0	79,8	0,98
	BF	91,5	93,9	0,97
5000	TF	42,9	43,6	0,98
	SC	48,8	50,1	0,97
	BF	55,6	57,3	0,97
6000	TF	30,0	30,7	0,98
	SC	33,5	34,4	0,97
	BF	37,4	38,5	0,97
7000	TF	22,2	22,8	0,98
	SC	24,4	25,1	0,97
	BF	26,8	27,7	0,97
8000	TF	17,1	17,6	0,97
	SC	18,6	19,2	0,97
	BF	20,2	20,9	0,97
9000	TF	13,6	14,0	0,97
	SC	14,6	15,1	0,97
	BF	15,8	16,3	0,97
10000	TF	11,1	11,4	0,97
	SC	11,8	12,2	0,97
	BF	12,6	13,1	0,96

LTB loads are calculated for qL and all units are the same as kilonewton. PE=Presented equation, AB= Abaqus, TF=Top flange, SC=Shear center, BF=Bottom flange, L=Beam-column length.

TABLE VIII
 SECTION A UNDER LOAD CASE 2 FOR $N/N_y=0.5$

L	Loading Position	PE	AB	PE/AB
4000	TF	58,6	55,9	1,05
	SC	67,5	64,4	1,05
	BF	77,8	74,2	1,05
5000	TF	37,8	36,4	1,04
	SC	42,5	40,9	1,04
	BF	47,7	45,9	1,04
6000	TF	26,5	25,7	1,03
	SC	29,2	28,3	1,03
	BF	32,2	31,1	1,03
7000	TF	19,6	19,1	1,03
	SC	21,3	20,7	1,03
	BF	23,2	22,5	1,03
8000	TF	15,1	14,7	1,03
	SC	16,3	15,9	1,03
	BF	17,5	17,1	1,03
9000	TF	12,0	11,7	1,02
	SC	12,8	12,5	1,02
	BF	13,7	13,4	1,02
10000	TF	9,8	9,6	1,02
	SC	10,4	10,2	1,02
	BF	11,0	10,8	1,02

LTB loads are calculated for qL and all units are the same as kilonewton. PE=Presented equation, AB= Abaqus, TF=Top flange, SC=Shear center, BF=Bottom flange, L=Beam-column length.

TABLE X
 SECTION B UNDER LOAD CASE 2 FOR $N/N_y=0.5$

L	Loading Position	PE	AB	PE/AB
4000	TF	45,8	51,1	0,90
	SC	47,3	52,7	0,90
	BF	58,6	64,4	0,91
5000	TF	29,0	31,6	0,92
	SC	29,8	32,4	0,92
	BF	35,4	38,2	0,93
6000	TF	20,0	21,4	0,93
	SC	20,5	21,9	0,93
	BF	23,6	25,1	0,94
7000	TF	14,6	15,5	0,94
	SC	14,9	15,8	0,95
	BF	16,9	17,8	0,95
8000	TF	11,2	11,7	0,95
	SC	11,3	11,9	0,95
	BF	12,6	13,2	0,95
9000	TF	8,8	9,2	0,96
	SC	8,9	9,3	0,96
	BF	9,8	10,2	0,96
10000	TF	7,1	7,4	0,96
	SC	7,2	7,5	0,96
	BF	7,8	8,2	0,96

LTB loads are calculated for qL and all units are the same as kilonewton. PE=Presented equation, AB= Abaqus, TF=Top flange, SC=Shear center, BF=Bottom flange, L=Beam-column length.

TABLE IX
 SECTION B UNDER LOAD CASE 2 FOR $N/N_y=0.25$

L	Loading Position	PE	AB	PE/AB
4000	TF	53,3	59,5	0,90
	SC	55,4	61,8	0,90
	BF	70,2	78,7	0,89
5000	TF	33,6	36,9	0,91
	SC	34,6	38,1	0,91
	BF	41,9	46,4	0,90
6000	TF	23,1	25,1	0,92
	SC	23,7	25,8	0,92
	BF	27,8	30,4	0,91
7000	TF	16,8	18,2	0,93
	SC	17,2	18,6	0,92
	BF	19,8	21,5	0,92
8000	TF	12,8	13,8	0,93
	SC	13,1	14,1	0,93
	BF	14,7	16,0	0,92
9000	TF	10,1	10,8	0,93
	SC	10,2	11,0	0,93
	BF	11,4	12,3	0,93
10000	TF	8,1	8,7	0,93
	SC	8,3	8,9	0,93
	BF	9,1	9,8	0,93

LTB loads are calculated for qL and all units are the same as kilonewton. PE=Presented equation, AB= Abaqus, TF=Top flange, SC=Shear center, BF=Bottom flange, L=Beam-column length.

Results in Tables IX, X have shown that LTB loads of section A and section B with different slendernesses subjected to uniformly distributed load calculated using presented equation are in good accordance with ABAQUS results.

IV. CONCLUSION

This paper presents a compact closed-form equation based on Ritz Method in order to evaluate LTB behavior of beam-columns with monosymmetric section subjected to constant axial force and various transverse load cases. The effect of axial loads, slenderness and loading positions on LTB loads of beam-columns are investigated by using proposed equation. Abaqus finite element software was utilized to validate LTB loads obtained by presented equation. It can be concluded that the results obtained by presented equation are in good accordance with ABAQUS results for low axial load level ($N/N_y=0-N/N_y=0.5$). Thus, proposed formula can be safely used in design of beam-column members under small axial load. However, buckling loads calculated using presented equation have become more conservative than abaqus solution due to the fact that the increase in axial load level after value of $N/N_y=0.5$ voids the assumption for minor axis bending which are used for the derivation of the proposed closed-form equation.

REFERENCES

- [1] M.A.M. Torkamani, E.R. Roberts, "Energy Equations for Elastic Flexural-Torsional Buckling Analysis of Plane Structures", Thin Walled Structures, vol. 47, no.4, pp. 463-473, 2009.
- [2] A. Chajes, *Principles of Structural Stability Theory*, Englewood Cliffs NJ, Prentice-Hall, 1974.
- [3] S. P. Timoshenko, J. M. Gere, *Theory of Elastic Stability*. 2nd ed., McGraw-Hill, New York, 1961.
- [4] W. F. Chen, E. M. Lui, *Theory of Beam-Columns vol.2 Space Behavior and Design*, McGraw-Hill, New York, 1977.
- [5] W. F. Chen, E. M. Lui, *Structural Stability: Theory and Implementation*, Elsevier Science Publishing Co. Inc., New York, 1987.

- [6] T.V. Galambos, A. E. Surovek, *Structural Stability of Steel: Concepts and Application for Structural Engineers*, John Wiley and Sons, 2008.
- [7] C. H. Yoo, S. C. Lee, *Stability of structures, principles and applications*, Elsevier, Oxford, 2011.
- [8] Z. P. Bazant, L. Cedolin, *Stability of Structures Elastic, Inelastic Fracture and Damage Theories*, Dover Publications, New York, 1991.
- [9] N. S. Trahair, *Flexural-Torsional Buckling of Structures*, CRC Press, London, 1993.
- [10] M. G. Salvadori, *Lateral buckling of eccentrically loaded I columns*, Transactions of the ASCE, vol. 121, pp. 1163–1178, 1956.
- [11] H. N. Hill, J. W. Clark, *Lateral buckling of eccentrically loaded I-section columns*, Transactions of the ASCE, vol. 116, pp. 1179, 1951.
- [12] F. Bleich, *Buckling Strength of Metal Structures*, McGraw Hill, New York, 1952.
- [13] M. Assadi, C. W. Roeder, “*Stability of Continuously Restrained Cantilevers*”, Journal of Engineering Mechanics, vol. 111, no. 12, pp. 1440–1456, 1985.
- [14] M. A. Serna, A. Lopez, I. Puente, D. J. Yong, “*Equivalent Uniform Moment Factors for Lateral-Torsional Buckling of Steel Members*”, Journal of Constructional Steel Research, vol. 62, no. 6, pp. 566–580, 2006.
- [15] B. Suryoatmono, D. Ho, “*The Moment-Gradient Factor in Lateral-Torsional Buckling on Wide Flange Steel Sections*”, Journal of Constructional Steel Research, vol. 58, no. 9, pp. 1247–1264, 2002.
- [16] S. Kitipornchai, N. J. Richter, “*Elastic Lateral Buckling of I-Beams with Discrete Intermediate Restraints*”, Civil Eng. Trans., vol. 20, no. 2, pp. 105–111, 1978.
- [17] S. Kitipornchai, P. F. Dux, N. J. Richter, “*Buckling and Bracing of Cantilevers*”, Journal of the Structural Division, ASCE, vol. 110, no. 9, pp. 2250–2262, 1984.
- [18] S. Kitipornchai, C. M. Wang, N. S. Trahair, “*Buckling of Monosymmetric I Beams under Moment Gradient*”, Journal of Structural Engineering, ASCE, vol. 112, no. 4, pp. 781–799, 1986.
- [19] S. Kitipornchai, N. S. Trahair, “*Buckling of Inelastic I-Beams under Moment Gradient*”, Journal of the Structural Division, ASCE, vol. 101, no. ST5, pp. 991–1004, 1975.
- [20] R.S. Barsoum, R.H. Gallagher, “*Finite Element Analysis of Torsional and Torsional-Flexural Stability Problems*”, International Journal of Numerical Methods in Engineering, vol. 2, no. 3, pp. 335–352, 1970.
- [21] G. Powell, R. Klingner, “*Elastic Lateral Buckling of Steel Beams*”, ASCE Journal of Structural Division, vol. 96, no. 9, pp. 1919–32, 1970.
- [22] G.J. Hancock, N.S. Trahair, “*Finite Element Analysis of Lateral Buckling of Continuously Restrained Beam-Columns*”, Civil Eng. Trans. Institution of Engineering, Australia, vol. CE20, no. 2, pp. 120–127, 1978.
- [23] M.A. Bradford, H.R. Ronagh, “*Generalized Elastic Buckling of Restrained I-Beams by FEM*”, ASCE Journal of Structural Engineering, vol. 123, no. 12, pp. 1631–1637, 1997.
- [24] J.P. Papangelis, N.S. Trahair, G.L. Hancock, “*Elastic Flexural-Torsional Buckling of Structures by Computer*”, Computers and Structures, vol. 68, no. 13, pp. 125–37, 1998.
- [25] H. Lee, D.W. Jung, J. H. Jeong, S. Im, “*Finite Element Analysis of Lateral Buckling for Beam Structures*”, Computers and Structures, 53(6), 1357–1371, 1994.
- [26] F. Mohri, A. Eddinari, N. Damil, M. Potier-Ferry, “*A Beam Finite Element for Non-linear Analyses of Thin-Walled Elements*”, Thin Walled Structures, vol. 46, no. 7-9, pp. 981–990, 2008.
- [27] J.S. Park, J.M. Stallings, Y.J. Kang, “*Lateral-Torsional Buckling of Prismatic Beams with Continuous Top-Flange Bracing*”, Journal of Constructional Steel Research, vol. 60, no.2, pp. 147–160, 2004.
- [28] N.H. Lim, N.H. Park, Y.J. Kang, I.H. Sung, “*Elastic Buckling of I-Beams under Linear Moment Gradient*”, International Journal of Solids and Structures, vol. 40, no. 21, pp. 5635–5647, 2003.
- [29] J.X. Gu, S.L. Chan, “*A Refined Finite Element Formulation for Flexural and Torsional Buckling of Beam-Columns with Finite Rotations*”, Engineering Structures, vol. 27, pp. 749–759, 2005.
- [30] H.R. Naderian, H.R. Ronagh, “*Buckling Analysis of Thin-Walled Cold-Formed Steel Structural Members Using Complex Finite Strip Method*”, Thin-Walled Structures, vol. 90, pp. 74–83, 2015.
- [31] S. Adany, B.W. Schafer, “*Generalized Constrained Finite Strip Method for Thin-Walled Members with Arbitrary Cross Section: Primary Modes*”, Thin-Walled Structures, vol. 84, pp. 150–159, 2014.
- [32] H.C. Bui, “*Semi-Analytical Finite Strip Method Based on The Shallow Shell Theory in Buckling Analysis of Cold-Formed Sections*”, Thin-Walled Structures, vol. 50, pp. 141–146, 2012.
- [33] H.C. Bui, “*Buckling Analysis of Thin-Walled Sections under General Loading Conditions*”, Thin-Walled Structures, vol. 47, pp. 730–739, 2009.
- [34] H. Ozbasaran, “*A Parametric Study on Lateral Torsional Buckling of European IPN and IPE cantilevers*”, International Journal of Civil, Architectural, Structural and Construction Engineering, World Academy of Science, Engineering and Technology, vol. 8, no. 7, 2014.
- [35] C. M. Wang, S. Kitipornchai, “*On Stability of Monosymmetric Cantilevers*”, Engineering Structures, vol. 8, pp. 168–180, 1986.
- [36] R. Aydin, A. Gunaydin, N. Kirac, H. Ozbasaran, “*On the Evaluation of Critical Lateral Buckling Loads of Prismatic Steel Beams*”, Proceedings of the Fourteenth International Conference on Civil, Structural and Environmental Engineering Computing, Civil-Comp Press, Stirlingshire, Scotland, 2013.
- [37] EC3, EN 1993-1-1, “*Eurocode 3: Design of Steel Structures-Part 1-1: General Rules and Rules for Buildings*”, European Committee for Standardization, Brussels, 2005.
- [38] AISC, “*Specification for Structural Steel Buildings, American Institute of Steel Construction*”, Chicago, 2005
- [39] F. Mohri, A. Brouki, J.C. Roth, “*Theoretical and Numerical Stability Analyses of Unrestrained, Mono-Symmetric Thin-Walled Beams*”, Journal of Constructional Steel Research, vol. 59, no. 1, pp. 63–90, 2003.
- [40] N. Kirac, T. Yilmaz, “*A Parametric Study on the Evaluation of Lateral Torsional Buckling of European IPE and IPN Beams*”, Proceedings of the Fifteenth International Conference on Civil, Structural and Environmental Engineering Computing, Stirlingshire, Scotland, 2015.
- [41] A. Andrade, D. Camotim, and P. Providência e Costa, “*On the evaluation of elastic critical moments in doubly and singly symmetric I-section cantilevers*”, Journal of Constructional Steel Research, vol. 63, pp. 894–908, 2007.
- [42] H. Ozbasaran, R. Aydin, M. Dogan, “*An Alternative Design Procedure for Lateral-Torsional Buckling of Cantilever I-Beams*”, Thin-Walled Structures, vol. 90, pp. 235–242, 2015.
- [43] W. Yuan, B. Kim, C. Chen, “*Lateral-torsional buckling of steel web tapered tee-section cantilevers*”, Journal of Constructional Steel Research, vol. 87, pp. 31–37, 2013.
- [44] B. Kim, L. Li, A. Edmonds, “*Analytical Solutions of Lateral-Torsional Buckling of Castellated Beams*”, International Journal of Structural Stability and Dynamics, vol. 16, pp. 155044, 2016.
- [45] L. Zhang, G. Tong, “*Lateral buckling of simply supported C- and Z-section purlins with top flange horizontally restrained*”, Thin-Walled Structures, vol. 99, pp. 155–167, 2016.
- [46] B. Asgarian, M.Soltani, F. Mohri, “*Lateral-torsional buckling of tapered thin-walled beams with arbitrary cross-sections*”, Thin-Walled Structures, vol. 62, pp. 96–108, 2013.
- [47] C. M. Wang, S. Kitipornchai, “*New set of buckling parameters for monosymmetric beam-columns/tie-beams*”, Journal of Structural Engineering, vol. 115, no. 6, pp. 1497–1513, 1989.
- [48] E. Magnucka-Blandzi, “*Critical State of a Thin walled beam under combined load*”, Applied Mathematical Modelling, vol. 33, pp. 3093–3098, 2009.
- [49] S. Cheng, B. Kim, L. Li, “*Lateral-torsional buckling of cold-formed channel sections subject to combined compression and bending*”, Journal of Constructional Steel Research, vol. 80, pp. 174–180, 2013.
- [50] M. Kucukler, L. Gardner, L. Macorini, “*Flexural-torsional buckling assessment of steel beam-columns through a stiffness reduction method*”, Engineering Structures, vol. 101, pp. 662–676, 2015.
- [51] ABAQUS, “*ABAQUS Theory Guide*”, Version 6.13.1, 2013.